

Matthew D. Eastin*
 Colorado State University, Fort Collins, CO

1. INTRODUCTION

Eyewall convection has long been recognized to play a crucial role in the evolution of hurricanes, but the particular forces driving the convection are widely debated. Malkus and Riehl (1960) first hypothesized that a few isolated buoyant "hot towers" must accomplish a large fraction of the required vertical mass and energy transport. In contrast, Emanuel (1986) demonstrated that symmetric hurricane-like vortices can be spun-up and maintained in a neutral environment. Zhang et al. (2000) further argued that the symmetric eyewall is primarily driven by the dynamically induced perturbation pressure gradient force. Soundings obtained near eyewall convection tend to support a near neutral stratification. However, direct observations of buoyancy within eyewall updrafts have been limited due to instrument wetting errors and difficulty in defining the appropriate background environment. In this study, we effectively account for these limitations and examine the buoyancy characteristics of eyewall convective updrafts.

2. DATA AND METHODS

The data consists of 175 radial legs obtained from 14 intense hurricanes at levels ranging from 850 to 500 mb. Each radial leg contains storm-relative observations of three-dimensional winds in cylindrical coordinates, temperature, dewpoint, geopotential height, and cloud water content partitioned in 0.5 km bins. The thermodynamic data was further processed to effectively remove instrument wetting errors (Eastin et al. 2002). Radial profiles of precipitation water content were derived from near-aircraft tail radar reflectivity values.

Total buoyancy, as defined by Houze (1993), is

$$B = g \left[\frac{\theta'_v}{\theta_v} + (K - 1) \frac{p'}{p} - q'_l \right] \quad (1)$$

$$B = TB + DB + WL \quad (2)$$

where primes represent deviations from a background environment (overbars). The three terms in (1) are referred to as thermal buoyancy (TB), dynamic buoyancy (DB), and water-loading (WL),

* *Corresponding Author Address:* Matthew D. Eastin, Department of Atmospheric Science, Colorado State University, Fort Collins, CO 80523; e-mail: eastin@atmos.colostate.edu

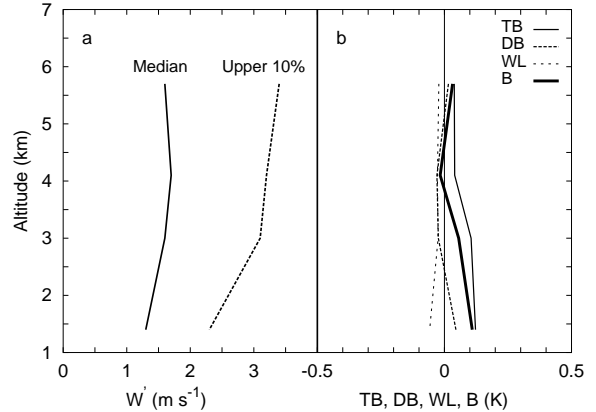


Figure 1: (a) Profiles of median \bar{w}' and the upper 10 percent values, and (b) median TB, DB, WL, and B for eyewall updraft cores. Note that vertical accelerations have been converted to units of K by dividing by g and multiplying by θ_v .

respectively. The key to examining buoyancy is to effectively separate the background balanced state from any locally unbalanced state. Recognizing that the hurricane's symmetric mesoscale structure is close to both hydrostatic and gradient balance, and that low-wavenumber asymmetries are in hydrostatic balance, we apply a 20 km running Bartlett filter to the thermodynamic data of each radial leg in order to represent the background mesoscale environment. The same filter is also applied to the vertical velocity data to remove the slowly-evolving low-wavenumber component from the transient convective features. Note that the perturbation total liquid water content (cloud + precipitation) is used in (1) since low-wavenumber components of q_l contribute to hydrostatic balance.

Convective updraft cores are defined from the perturbation vertical velocity (w') as radial segments with $w' > 1$ m/s for at least 0.5 km. A total of 351 cores were identified within the eyewall region, which was subjectively determined from radar for each leg. The altitude, diameter (DIAM), average vertical velocity (\bar{w}'), TB, DB, WL, and B were tabulated for each core, and distributions of each parameter were constructed for each altitude.

3. RESULTS AND DISCUSSION

The distributions of \bar{w}' and DIAM at each level (not shown) are linear on log-normal probability plots, and distributions of TB, DB, WL, and B (not

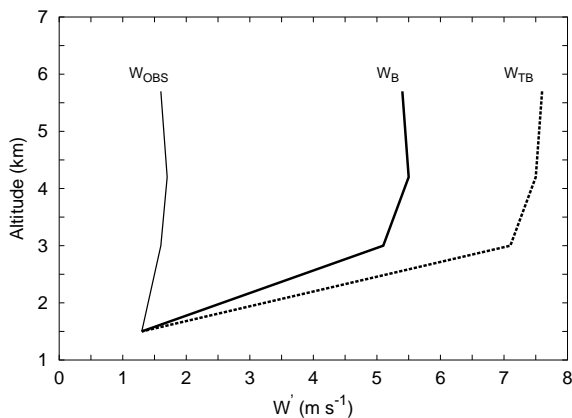


Figure 2: Profiles of eyewall observed median \bar{w}' (W_{OBS}), and calculated \bar{w}' from median B (W_B) and TB (W_{TB}) values.

shown) are roughly Gaussian in agreement with previous studies. The vertical profiles of the median and upper 10% \bar{w}' (Fig. 1a) indicate that *typical* eyewall convective updrafts experience modest acceleration at the lower and middle levels. The vertical profiles of median TB, DB, WL, and B (Fig. 1b) suggest that *typical* eyewall updrafts are slightly buoyant, particularly at lower levels. Although the median B values are small, one must remember that the distribution represents convection at all stages of its life-cycle. Numerous updraft cores contain B values in excess of $50 \text{ m s}^{-1} \text{ h}^{-1}$ ($\theta'_v \sim 0.5 \text{ K}$).

We can elucidate the role of buoyancy in driving typical eyewall convection by a simple updraft model. If we assume an updraft experiences no lateral mixing or forcing during its ascent the vertical momentum equation can be written as

$$\frac{dw'}{dz} = \frac{1}{w'} \left[\frac{1}{\rho} \frac{dp'}{dz} + B \right] \quad (3)$$

where the first term inside the brackets is the vertical perturbation pressure gradient force (VPGF). To derive the vertical profile of expected \bar{w}' from buoyancy alone, we neglect the VPGF in (3) and integrate from $z = 1.5 \text{ km}$ upward, using the median TB and B profiles. The median \bar{w}' at $z = 1.5 \text{ km}$ is used as a lower boundary condition. The resulting profiles (Fig 2) have similar vertical structures as the profile of observed updrafts, but indicate that buoyancy itself will produce much stronger updrafts. One can thus infer that the net VPGF typically acts to *decelerate* updrafts. One can also infer that decelerations by the VPGF and WL (profile from TB only) are of the same order of magnitude. It is interesting to note that a modest positive correlation ($r = 0.33$) between \bar{w}' and TB was found at 500 mb, suggesting that the *majority* of strong convective updrafts at this level have accelerated via buoyancy.

Table 1: Percentage of net upward mass transport in the eyewall region accomplished by convective updrafts cores with certain characteristics.

Height (km)	$\bar{w}' > 2.0$	$\bar{w}' > 3.0$	B > 0	B > 25
5.7	42%	24%	43%	31%
4.2	59%	28%	47%	25%
3.0	40%	22%	29%	13%
1.5	19%	13%	38%	20%
Mean	42%	23%	37%	21%

Next, we can elucidate the role of buoyant convective updrafts within the hurricane's secondary circulation by the fraction of net upward mass transport they accomplish. This fraction was calculated by dividing the summed mass transport ($\rho \bar{w}' \text{DIAM}$) in the desired convective cores by the summed net mass transport within the eyewall region of all legs. The results for various core criteria (Table 1) indicate that strong and buoyant convective eyewall cores accomplish up to $\sim 40\%$ of the vertical transport in the secondary circulation, and that the percentage tends to increase with height. It should be noted that buoyant convective updrafts occupy only 5% of the total eyewall region area, and that strong convective updrafts occupy a similar area.

The results presented here suggest that typical eyewall convective updrafts are driven by buoyancy forces, but are moderated by water-loading and vertical perturbation pressure gradient forces. Furthermore, strong and buoyant updraft cores may occupy only a small fraction of the eyewall region, but they accomplish a significant fraction of the net vertical transport. These results support the "hot tower" hypothesis. How then can a symmetric representation of a hurricane-like vortex develop and maintain itself without buoyancy? The answer likely lies in either the azimuthal distribution of convective updrafts and downdrafts that comprise the mean eyewall, or how symmetric models account for asymmetric processes. Results concerning the spatial distribution of strong and buoyant updraft cores, and their source, will be presented at the conference.

Acknowledgments: I wish to thank HRD for providing access to the data and William Gray for his support. Funding was provided by NSF Grant No. ATM-9616818.

REFERENCES

- Eastin, M. D., P. G. Black, and W. M. Gray, 2001: Flight-level instrument wetting errors in hurricanes. Part I: Observations. *Mon. Wea. Rev.*, 130, 825-841.
- Emanuel, K. A., 1986: An air-sea interaction theory for tropical cyclones. Part I: Steady-state maintenance. *J. Atmos. Sci.*, 43, 585-604.
- Houze, R., 1993: *Cloud Dynamics*, Academic Press, 573 pp.
- Malkus, J., and H. Riehl, 1960: On the dynamics and energy transformations in steady-state hurricanes. *Tellus*, 12, 1-20.
- Zhang, D.-L., Y. Liu, and M. K. Yau, 2000: A multiscale numerical study of Hurricane Andrew (1992). Part III: Dynamically induced vertical motion. *Mon. Wea. Rev.*, 128, 3772-3788.